Preliminary study on the differentiation of vulnerable carotid plaques via analysis of calcium content and spectral curve slope by using gemstone spectral imaging

ZE-XIN FAN[1], SHAO-JIE YUAN[2], XIAO-QING LI[1], TING-TING YANG[1], TIAN-TONG NIU[1], LIN MA[1], KAI SUN[3], LI WANG[2] and GUANG-ZHI LIU[1]

[1]Department of Neurology, Beijing Anzhen Hospital, Capital Medical University, Beijing 100029; Departments of [2]Neurology and [3]Imaging, Second Hospital of Shanxi Medical University, Taiyuan, Shanxi 030001, P.R. China

Received November 2, 2021; Accepted February 23, 2022

DOI: 10.3892/etm.2022.11254

Abstract. Growing evidence indicates that vulnerable carotid plaque rupture is an important cause of stroke. However, the role of novel gemstone spectral imaging (GSI) in the assessment of vulnerable carotid plaques has remained to be sufficiently explored. Therefore, the aim of the present study was to provide a comprehensive evaluation of carotid atherosclerotic plaques using both GSI imaging biomarkers and serological biomarkers, and further explore their possible roles in the atherogenic process. The present study analyzed GSI data, including calcium content of carotid atherosclerotic plaques and spectral curve slope, as well as serum high-sensitivity C-reactive protein (Hs-CRP) and monocyte chemotactic protein-1 (MCP-1) levels in patients with a carotid atherosclerotic plaque using GSI-computed tomographic angiography and immunoturbidimetry. Patients with unstable plaque exhibited a significantly lower calcium content and higher spectral curve slope than those of the stable plaque group. In addition, patients with unstable plaque exhibited an increase in Hs-CRP and MCP-1 levels compared with those of the stable plaque and normal control groups. The alteration in GSI calcium content and spectral curve slope reflects a close link between calcification and plaque instability, while aberrant Hs-CRP and MCP-1 expression are involved in the formation or development of vulnerable plaques. Taken together, the present results strongly support the feasibility of using these serological and newly identified imaging parameters as multiple potential biomarkers relevant to plaque vulnerability or stroke progression.

Correspondence to: Dr Guang-Zhi Liu, Department of Neurology, Beijing Anzhen Hospital, Capital Medical University, 2 Anzhen Road, Beijing 100029, P.R. China
E-mail: guangzhi2002@hotmail.com

Abbreviations: GSI, gemstone spectral imaging; Hs-CRP, high-sensitivity C-reactive protein; MCP-1, monocyte chemoattractant protein-1; LRNC, lipid-rich necrotic core; IPH, intraplaque hemorrhage; CT, computed tomography; MRI, magnetic resonance imaging; CTA, computed tomographic angiography; MRA, magnetic resonance angiography; MD, material decomposition; ROI, region of interest; TIA, transient ischemic attack; ROC, receiver operating characteristic; CEA, carotid endarterectomy; CAS, carotid artery stenting

Key words: gemstone spectral imaging, high-sensitivity C-reactive protein, monocyte chemotactic protein-1, plaque vulnerability

Introduction

Atherosclerosis is a lipid-driven chronic disease that leads to plaque formation in the arterial wall through intimal inflammation, necrosis, fibrosis and calcification. As one of the critical factors of ischemic stroke, an atherosclerotic carotid plaque contains a lipid-rich necrotic core (LRNC), areas of intraplaque hemorrhage (IPH), calcification and fibrous components, and vulnerable carotid plaques tend to consist of an LRNC and areas of IPH, rather than of calcification and fibrous components. Of note, growing evidence indicates that vulnerable plaque rupture, beyond perfusion defects caused by luminal stenosis, is an important cause of stroke (1). Two distinct studies reported that in patients with mild to moderate stenosis, vulnerable plaques were associated with the occurrence of subsequent cerebrovascular events, which was markedly higher than in patients with severe stenosis (>70%) (2,3). Furthermore, a previous histopathologic assessment also suggested that certain plaque elements known as hallmarks of unstable plaque, independent of arterial narrowing, were more likely to cause cerebrovascular or cardiovascular disorders (4). Thus, when designing therapeutic interventions for effective stroke prevention, it is crucial to identify carotid atherosclerotic plaques and high-risk determinants as early as possible.

So far, various plaque imaging techniques [ultrasound, computed tomography (CT) and magnetic resonance imaging (MRI)] and serological biomarkers of vulnerability [high-sensitivity C-reactive protein (Hs-CRP), MMP-9 and sCD40 ligand] have been adopted to predict the risk of cerebrovascular events (5). In addition, as a key chemokine, monocyte chemotactic protein-1 (MCP-1) has been demonstrated to have

important roles in atherosclerosis by promoting the migration and infiltration of monocytes into the plaque through its receptor C-C motif chemokine receptor 2 (6). Among the neuroimaging technologies, a novel gemstone spectral imaging (GSI) technique that incorporates CT angiography (CTA) with a gemstone detector has received increasing attention in recent years (7). Although conventional CT and CTA have been widely used for quantitative measurement of tissue composition and grading of the severity of stenosis in patients with stroke, they exhibit deficiencies in the ability to characterize different components of mixed or noncalcified plaques, particularly in smaller plaques and vessels. Unlike conventional CT and CTA, GSI further improves the characterization and quantification of plaque components, since it collects data using multiple single-source spectra to generate additional material-differentiating information via the combination of CT techniques with the measurement of spectral attenuation properties of the examined tissue to achieve material decomposition (MD).

Hence, GSI holds great potential to better characterize and quantify the concentration of plaque components, such as lipids, calcification and fibrous tissues (8), in order to accurately distinguish vulnerable plaques from stable plaques in carotid arteries. A recent study by Shinohara *et al* (9) compared the applicability of GSI to that of 3D time-of-flight magnetic resonance angiography (MRA) in patients with carotid artery stenosis, revealing that the effective Z-value of noncalcified carotid plaques was markedly lower in the group with high signal intensity than that in the group with low signal intensity on MRA. Taken together with another study revealing a high concordance between GSI and virtual histology-intravascular ultrasound in the assessment of carotid plaque composition using effective Z-maps (10), these findings indicate the potential use of GSI for the identification of vulnerable carotid plaques. Therefore, the aim of the present study was to provide a comprehensive evaluation of carotid atherosclerotic plaques using both GSI imaging biomarkers and serological biomarkers, and further explore their possible roles in the atherogenic process. GSI-CTA data, as well as serum Hs-CRP and MCP-1 levels were analyzed in patients with this disease in an attempt to establish a novel strategy for the comprehensive assessment of vulnerable carotid plaques by integrating the GSI variables along with the serological parameters.

Patients and methods

Subjects. A total of 42 cases of asymptomatic carotid plaque (27 males and 15 females; mean age, 63.6±10.4 years) were enrolled in the present study. All patients were diagnosed based on their medical history, clinical examination and results of carotid duplex sonography, brain MRI and MRA scans. Ultrasound assessment was performed for carotid artery segmentation, in which the carotid artery was divided into four different segments: i) Common carotid artery, ii) carotid bulb, iii) external carotid artery and iv) internal carotid artery. Carotid plaques were detected by ultrasound and characterized according to the Mannheim consensus as focal structures encroaching into the arterial lumen by ≥0.5 mm or 50% of the surrounding intima-media thickness value, or a thickness ≥1.5 mm (11). Furthermore, these patients with carotid plaques underwent GSI scan and were then further divided into an unstable plaque group (n=17; 5 males and 12 females; mean age, 63.29±11.91 years) and stable plaque group (n=25; 10 males and 15 females; mean age, 63.80±9.57 years). A total of 19 healthy individuals (10 males and 9 females; mean age, 60.3±11.8 years), who received carotid ultrasound examination and exhibited no large-vessel atherosclerosis, were included as normal controls (NCs). The study protocol was reviewed and approved by the Ethics Committee of Beijing Anzhen Hospital (Beijing, China). All diagnostic procedures were performed in accordance with relevant guidelines and regulations, and written informed consent was obtained from all of the participants of the study.

None of the participating individuals had i) stroke, myocardial infarction, brain tumors, blood diseases or other abnormal coagulation diseases, rheumatic heart disease, infectious endocarditis, arrhythmia, serious liver or kidney diseases, acute or chronic inflammatory diseases or autoimmune diseases; ii) disturbance of consciousness or severe cognitive impairment; nor iii) other reasons to prevent them from undergoing GSI. The following diagnostic tests were performed in both patients and NCs: Complete blood count, blood chemistry, Hs-CRP, electrocardiogram, posterior-anterior chest radiography, transthoracic cardiac echocardiography, transcranial Doppler ultrasonography and carotid duplex sonography.

Sample collection. Whole blood samples were drawn between 9:00 a.m. and 12:00 p.m. After centrifugation, the serum was collected and stored at -70˚C in small aliquots for further use.

CT protocols. Upon injection of nonionic contrast agent (iopamidol; Bracco Imaging), GSI-CTA was performed with a scan delay of 5 sec using a 64-slice spiral CT scanner with a gemstone detector (GE Discovery CT 750 HD; GE Healthcare). The flow rates and volume of contrast material were determined based on a fixed duration (12 sec) of injection and dose tailored to the bodyweight of each patient (252 mgI/kg). A total of 65 ml iopamidol (30 gI/100 ml) was intravenously injected at a flow rate of 3.5 ml/sec, followed by administration of 30 ml saline chaser at the same flow rate. Scanning was performed using the 0.6x0.625 mm GSI mode. The scanning parameters employed in GSI mode were as follows: Tube voltage, 80/140 kV and 0.5-msec instantaneous switch; tube current, 600 mA; slice thickness, 0.625 mm; rotation speed, 0.8 sec; helical pitch, 1.375; and matrix, 512x512.

Image evaluation. After scanning, GSI viewer 4.5 (GE Healthcare) was utilized for further analysis. GSI plaque imaging was initially quantified for carotid atherosclerotic plaque characterization. The images were reviewed in a blinded fashion by two radiologists who are experts in carotid plaque imaging. They participated in the interpretation of the data, discussing and reaching a consensus if any disagreement occurred. To avoid potential radiation damage to X-ray-sensitive organs such as the lens and thyroid gland in the head and neck, the middle part of the ascending aorta was selected as the region of interest (ROI), where a threshold

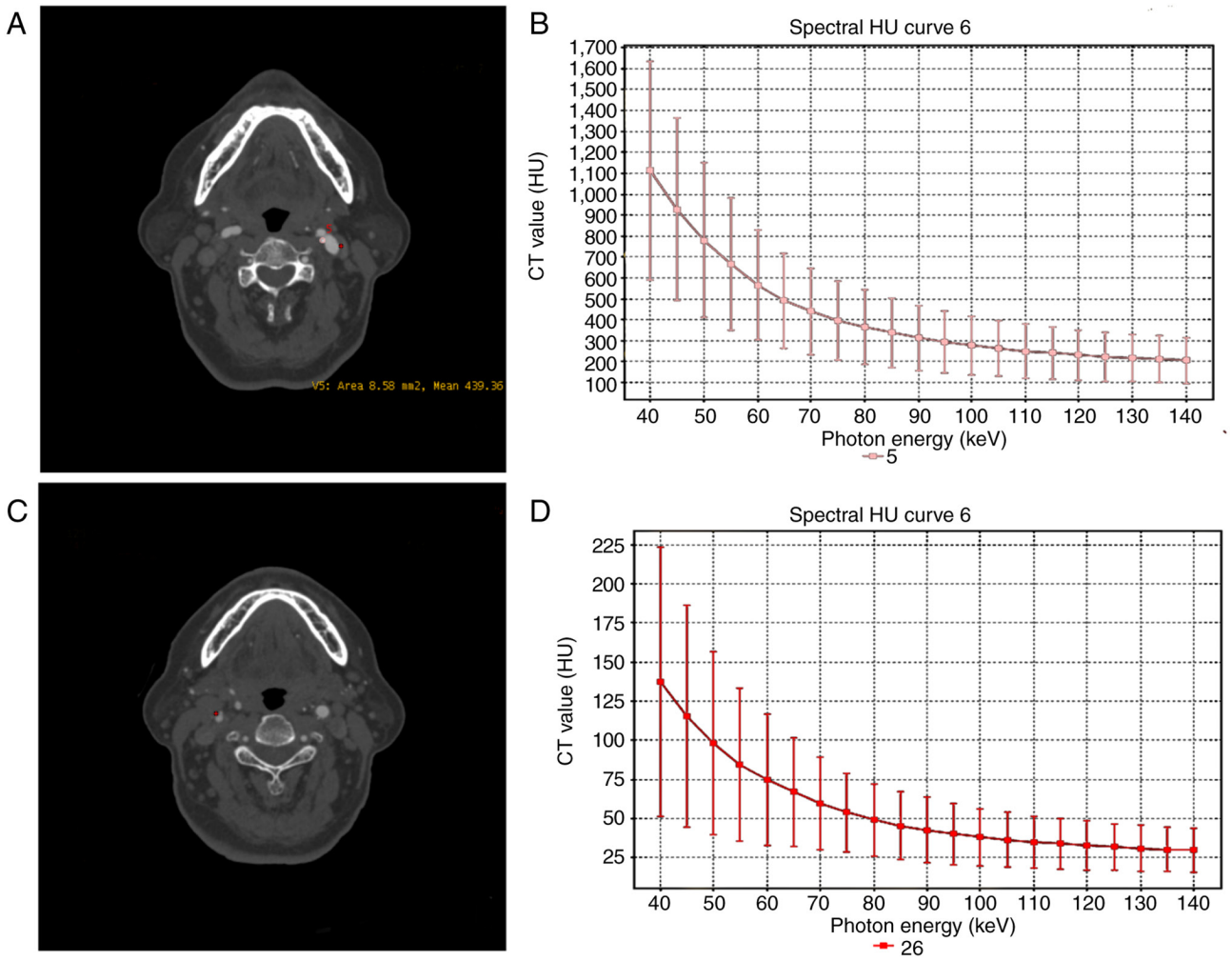

Figure 1. Gemstone spectral imaging of carotid plaque in a 64-year-old woman. (A) CTA source image presents a calcified plaque (indicated by pink dot). (B) Plaque energy spectrum shows a bow curve with negative slope and CT value >220 HU. (C) CTA source image presents a fibrous plaque (indicated by red cross). (D) Plaque energy spectrum displays a bow curve with negative slope and CT value between 30 and 150 HU. CTA, computed tomographic angiography; HU, hounsfield units.

value of 100 Hounsfield units (HU) was established for triggering the contrast-enhanced scan (12). The area of ROI is ~10 mm^2. The minimum ROI volume was set on the plaque through post-processing techniques and a characteristic spectral attenuation curve in HU of the corresponding region was acquired. The points on the curve represent the average CT values of tissues at different keV levels.

The ROI was then placed in the fat tissue, muscle fiber tissue and bone structure, and three distinctive attenuation curves with different colors were obtained to determine the nature of the plaques (Fig. 1). Three categories of plaques were defined according to their average CT values: i) Lipid cores plaques, non-calcified plaques (NCPs)<30 HU; ii) fibrous plaques, 30 HU<NCP<150 HU; and iii) calcified plaques, >220 HU. Furthermore, the calcified plaques were divided into spotty or large calcification. The former refers to plaques of <3 mm in size on curved multiplanar reformation images and 1-sided on axial images, while the latter refer to plaques with calcification greater than the spotty calcification (13). Large calcified and fibrous plaques were recognized as stable plaques, whereas lipid and spotty calcified plaques were regarded as unstable plaques (13,14).

Upon qualitative analysis of the atherosclerotic plaques, MD analysis was selected for measurement of the intraplaque calcium content. In brief, the energy range was set at 65 keV, followed by placing of the minimum ROI volume on the target plaque, ensuring that the ROI was placed on the images with the original scanning layer thickness, particularly those with a relatively uniform density, in order to detect the tissue content (g/l) of the corresponding intraplaque structure. Calcium (water)-based MD analysis was performed as described previously (15) to measure intraplaque calcium content in the selected ROI using an extracted calcium map. In addition, the slope of the spectral curve associated with the CT value of the plaque was calculated and the difference between the CT values of two measured points on the energy spectrum curve was divided by the energy difference between these two points. In the present study, since the single-energy CT values at 40 and 110 keV were selected as reference points, the value of the slope K of the spectrum curve was equivalent to (CTa-CTb)/70.

Immunoturbidimetry. Serum MCP-1 levels were determined with a commercial immunoturbidimeter (cat. no. EK0441;

Wuhan Boster Biological Technology, Co. Ltd.) according to the supplier's instructions, with a detection limit of 15.6 pg/ml. All assays were performed simultaneously in a blinded manner.

Follow-up. To explore the difference in short-term prognosis between stable and unstable plaques, trained investigators collected patients' data through telephone or face-to-face interviews at 1, 3 and 12 months after baseline measurements. Clinical events and medical therapy were evaluated at each follow-up visit among all patients. The primary outcome measures were a composite of stroke (either ischemic or hemorrhagic) or transient ischemic attack (TIA), whichever occurred first. All of the primary outcome events and medical therapies were reviewed by TTN and LM.

Statistical analysis. Statistical analysis was performed using GraphPad Prism 8 (GraphPad Software Inc.). Quantitative data are presented as the mean ± standard deviation (age, leukocyte, monocyte, calcium content, MCP-1 level) or as the median with interquartile range (Hs-CRP level and spectral curve slope). Normally distributed data were analyzed by one-way ANOVA for multiple-group comparison and the Student-Newman-Keuls post-hoc test for intergroup comparison, or with a Pearson's correlation test. Non-normally distributed data were analyzed with the Kruskal-Wallis test or Spearman's correlation analysis. The χ^2 test was used to compare differences in qualitative data (sex, diabetes, coronary artery disease, dyslipidemia, hypertension, smoking, peripheral artery disease and carotid stenosis) between groups. Receiver operating characteristic (ROC) curve analysis was also performed for quantitative slope of spectral curve, calcium content, serum Hs-CRP and MCP-1 level, and areas under the ROC curve (AUC) were calculated. P<0.05 was considered to indicate statistical significance.

Results

Baseline characteristics. Patient characteristics, including risk factors and laboratory data, obtained on the first day of sampling, are presented in Table I. No significant differences were observed between NCs and either of the carotid atherosclerosis groups.

Carotid atherosclerotic plaque characterization by using GSI. CTA source image presents a stable plaque in the left carotid bulb, and the energy spectrum curve of plaque displays a bow-down curve with a negative slope (Fig. 1). Among the 42 patients with carotid atherosclerosis, a total of 22 unstable plaques were detected in 17 cases, while a total of 30 stable plaques were detected in 25 cases by using GSI. In the unstable plaque group, the position of the atherosclerosis plaque was the carotid bulb (12/22, 54.5%), common carotid artery (5/22, 22.7%) and external carotid artery (5/22, 22.7%). In the stable plaque group, there were 15 cases in the carotid bulb (15/30, 50%), 8 cases in the common carotid artery (8/30, 26.7%) and 7 cases in the external carotid artery (7/30, 23.3%). However, no plaques were identified in the internal carotid artery in both carotid plaque groups. No significant differences in the location of the plaques in the different carotid segments were observed between the stable and unstable plaque groups (Fig. 2).

Calcium content in plaques and slope of spectral curve via GSI. In the selected ROI, the calcium content was significantly lower in the unstable plaque group (47.53±37.17 g/l) than in the stable plaque group (147.85±49.54 g/l; P<0.001), while the slope of the spectral curve was significantly higher in the unstable plaque group [0.29 (interquartile range: -3.86, 3.00)] than in the stable plaque group [-6.55 (interquartile range: -14.55, -4.50); P<0.001] (Fig. 3). Additional data are presented in Table SI.

Serum Hs-CRP and MCP-1 levels. Patients with unstable plaques exhibited increased Hs-CRP levels [15.33 (interquartile range: 10.65, 17.35) mg/l] compared with those of the stable plaque and NC groups [2.38 (interquartile range: 1.23, 3.75) mg/l and 1.21 (interquartile range: 0.76, 1.50) mg/l, respectively; both P<0.001]. Similarly, there were significantly elevated MCP-1 levels in patients with unstable plaques (467.13±66.28 pg/ml) compared with those in the stable plaque and NC groups (351.84±81.89 and 153.64±49.79 pg/ml, respectively; both P<0.001) (Fig. 3). Additional data are presented in Table SI.

ROC of calcium content, spectral curve slope and serum levels of Hs-CRP and MCP-1 in the plaque groups. In general, the ROC curves were constructed for calculation of the AUC at the optimal cut-off value along with maximum sensitivity and specificity. As a result, the generated AUC of the calcium content in carotid plaque was 0.938 and the assumed cut-off calcium content for discriminating stable and unstable plaque was 101.5 pg/ml, with a sensitivity of 73.33% and a specificity of 100%. The generated AUC of the slope of the spectral curve was 0.942 and the assumed cut-off slope of the spectral curve for differentiating stable from unstable plaque was 3.835, with a sensitivity of 96.67% and a specificity of 77.27%. The generated AUC of serum Hs-CRP was 1 and the optimal Hs-CRP threshold cutoff was determined to be 7.14 mg/l, with a sensitivity and specificity of 100 and 100%, respectively. The generated AUC of serum MCP-1 was 0.901 and the optimal MCP-1 threshold cutoff was determined to be 392.3 pg/ml, with a sensitivity and specificity of 84 and 100%, respectively (Fig. 4). Additional data are presented in Table SII.

Correlation analysis. Age, complete blood counts (leukocytes and monocytes) and calcium content were not significantly correlated with the serum levels of Hs-CRP or MCP-1 in either the patients or NC groups. No obvious correlation was observed between the calcium content, serum levels of Hs-CRP or MCP-1 in either patients with unstable plaques nor those with stable plaques (data not shown). No obvious correlation was obtained between the calcium content and spectrum curve slope in patients with unstable plaques (r=-0.236, P=0.291; data not shown), but the calcium content was significantly negatively correlated with spectrum curve slope in patients with stable plaques (r=-0.494, P=0.006) (Fig. S1).

Medication use and cerebrovascular events. During the 1-year follow-up, no significant differences were observed in the

Table I. Baseline characteristics of patients and NC.

Parameter	Unstable plaque (n=17)	Stable plaque (n=25)	NC (n=19)	P-value
Age, years	63.30±11.90	63.80±9.60	60.20±11.80	0.555
Female sex	12.00 (70.60)	15.00 (60.00)	10.00 (52.60)	0.543
Diabetes	3.00 (17.70)	5.00 (20.00)	-	0.849
Coronary artery disease	3.00 (17.70)	2.00 (8.00)	-	0.343
Hypercholesterolemia	10.00 (58.80)	9.00 (36.00)	4.00 (21.10)	0.064
Hypertension	7.00 (41.20)	9.00 (36.00)	-	0.735
Smoking	7.00 (41.20)	7.00 (28.00)	4.00 (21.10)	0.665
Peripheral artery disease	7.00 (41.20)	8.00 (32.00)	-	0.542
Leukocytes, $x10^3/\mu l$	7.01±2.12	7.06±1.65	6.86±1.92	0.935
Carotid stenosis, %				0.318
>50	6.00 (35.30)	11.00 (44.00)	-	
≤50	11.00 (64.70)	14.00 (56.00)		
Monocytes, $x10^3/\mu l$	0.39±0.11	0.38±0.09	0.35±0.10	0.450

Values are expressed as n (%) or the mean ± standard deviation. NC, normal controls.

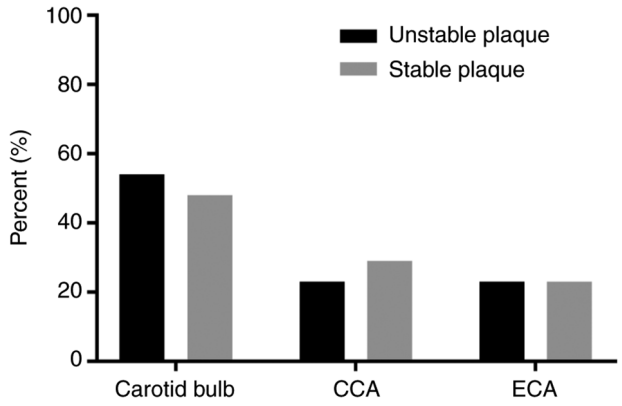

Figure 2. Different locations of plaques in the carotid artery. The distribution of unstable plaque and stable plaque in different carotid segments were compared. The vertical axis indicates the proportion of the plaque distribution. CCA, common carotid artery; ECA, external carotid artery.

medication use between the two carotid atherosclerosis groups, with the exception of higher use of lipid-lowering drugs in the unstable plaque group than in the stable plaque group (P<0.001). No deaths occurred in the present study cohort. Ischemic stroke occurred in 2 patients with unstable plaques (2/17, 11.8%) due to artery-to-artery embolism from the carotid artery origin and in 2 patients with stable plaques (2/25, 8%) in the absence of TIA or intracranial hemorrhage (Table II), but no statistically significant difference in the occurrence rate of ischemic stroke was obtained between these two groups (P>0.05).

Discussion

In the present study, patients with unstable plaques exhibited a decrease in calcium content compared with that of the calcified plaques group. Together with a previous study suggesting that less calcification was associated with clinically symptomatic plaques rather than with asymptomatic plaques (16), this finding indicates that the GSI calcium content may be associated with plaque instability. This is noteworthy because recent data have demonstrated that atherosclerotic plaque calcification is a complex, active biological process involving plaque vulnerability to rupture, consequently leading to major cardiovascular events such as myocardial infarction. At present, clinical imaging modalities, including non-invasive methods such as CT or invasive methods such as intravascular US or optical coherence tomography, are utilized for the characterization of calcified carotid plaques (17). To the best of our knowledge, the present study is the first time the GSI technique has been adopted to analyze the calcium content in carotid atherosclerotic plaque. In the present study, this novel technique was selected because, inheriting the detection sensitivity of CT towards calcium, GSI uses X-rays and expresses the absorption of the energy spectrum based on tissue composition and lesions, performing quantitative analysis via the MD technique, where the calcium map displays only calcium density and enables measurement of calcium content in plaques (7,8). Of note, the present study also indicated that the spectral curve slope of the CT value of the plaque in patients with stable plaques was significantly lower than that of patients with unstable plaques, which is in agreement with a previous study by Karçaaltıncaba and Aktaş (18), who reported that vulnerable plaques were rich in lipid cores and their energy spectrum curve exhibited a bow-up curve with a positive slope, whereas stable plaques had a bow-down curve with a negative slope. Of note, in the present study, ROC curve analyses were performed, which revealed the optimal diagnostic threshold values of calcium content and spectral curve slope for differentiating vulnerable from stable plaques, as well as their distinctive specificity and sensitivity, indicative of different roles of these parameters in the assessment of carotid plagues. Indeed, an obvious correlation was observed between the calcium content and spectrum curve slope in the patients with stable plaques, but not in the patients with unstable plaques, further supporting the present viewpoint. Taken together, the

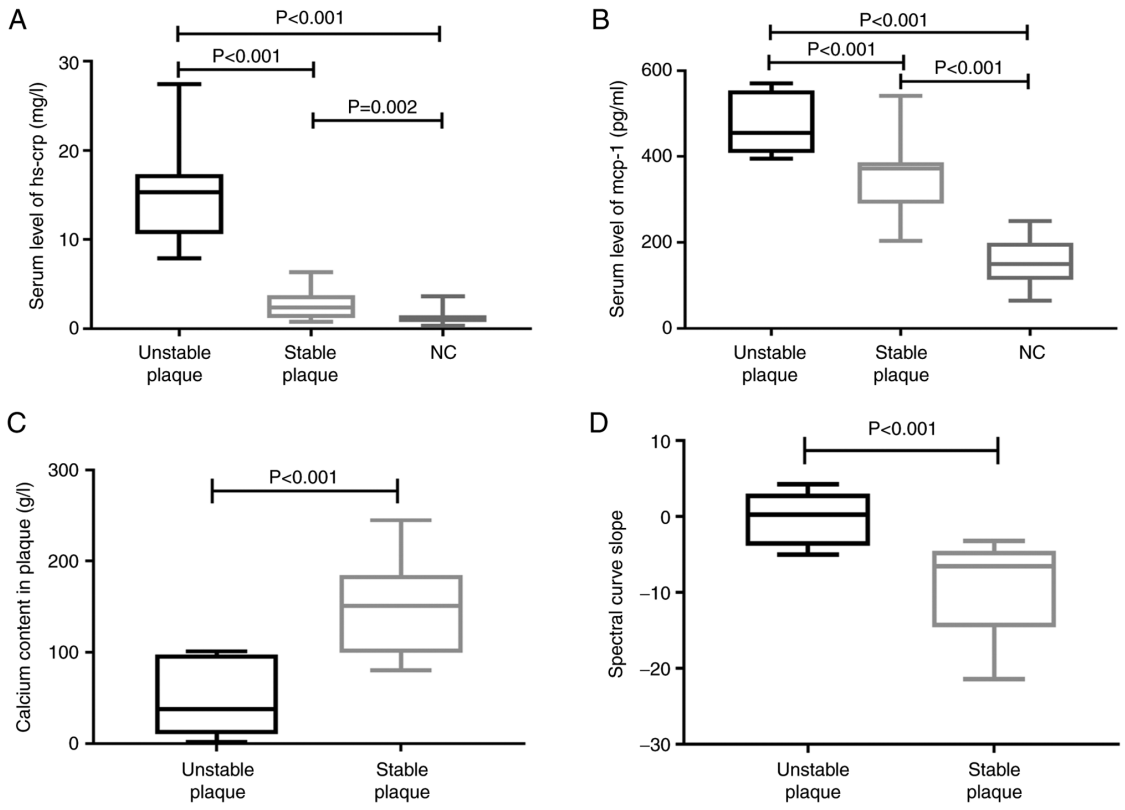

Figure 3. Serum levels of Hs-CRP and MCP-1 in the three groups, spectral curve slope and calcium content in the plaque groups. The serum levels of (A) Hs-CRP and (B) MCP-1 determined using immunoturbidimetry were compared among patients with stable plaques, unstable plaques and NC. (C) Calcium contents in plaque and (D) spectral curve slope of plaque are compared between patients with stable plaques and unstable plaques using gemstone spectral imaging. Horizontal lines indicate mean values with standard deviation or median values, while numerals on top are P-values. NC, normal controls; Hs-CRP, high-sensitivity C-reactive protein; MCP-1, monocyte chemotactic protein-1.

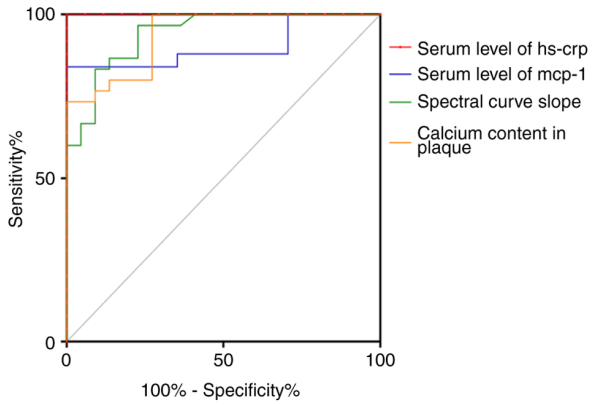

Figure 4. ROC curve analysis of spectral curve slope, calcium content in plaque and serum levels of Hs-CRP, MCP-1 in the plaque groups. Quantitative analysis for curve slope of plaque (green line), calcium content in plaque (orange line), serum MCP-1 level (blue line) and serum Hs-CRP level (red line) in plaque groups was performed using ROC curve analysis. The AUC for the calcium content in the plaque was 0.938 and the assumed cut-off for the calcium content for discriminating between stable and unstable plaque was 101.5 (g/l), with a sensitivity of 73.33% and a specificity of 100%. The AUC of the slope of the spectral curve was 0.942 and the assumed cut-off for the slope of the spectral curve for differentiating stable from unstable plaque was 3.835, with a sensitivity of 96.67% and a specificity of 77.27%. The AUC of serum Hs-CRP levels was 1 and the optimal Hs-CRP threshold cutoff was determined to be 7.14 mg/l, with associated sensitivity and specificity of 100 and 100%, respectively. The AUC of serum MCP-1 levels was 0.901 and the ideal MCP-1 threshold cutoff was determined to be 392.3 pg/ml, with associated sensitivity and specificity of 84 and 100%, respectively. ROC, receiver operating characteristic; AUC, area under the curve; Hs-CRP, high-sensitivity C-reactive protein; MCP-1, monocyte chemotactic protein-1.

present results indicated that these two GSI parameters may serve as potential imaging biomarkers relevant to plaque vulnerability or disease progression.

As the most promising indicator for vascular inflammation, CRP is one of the acute-phase proteins mainly produced in the liver during episodes of acute inflammation or infection. Hs-CRP assay methods are capable of detecting small changes in CRP concentrations. Hs-CRP is currently considered a predictor of future cardiovascular events and was classified as class III B level of evidence in the 2016 European guidelines on cardiovascular disease prevention (19), albeit controversy on the validity of this biomarker still exists. Various studies have provided strong evidence that CRP inhibits endothelial nitric oxide production and contributes to plaque instability by activating NF-κB, inducing the expression of MMP-2 and -9 (20). In line with these previous studies, the present study indicated that, compared with those in the stable plaque or NC groups, patients with unstable plaques had markedly elevated serum Hs-CRP levels. Furthermore, optimal diagnostic threshold values were also obtained for separating vulnerable from stable plaques with higher specificity and sensitivity than either calcium content or spectral curve slope, supporting the view that alterations in this inflammatory biomarker are closely associated with the formation or development of vulnerable carotid plaques. This is noteworthy, since a novel strategy for multiplying individual profiles has been proposed by Nederkoorn (21) for the selection of patients with the highest risk and for the selection of the best treatment. For

Table II. Medication use and cerebrovascular events during 1-year follow-up in the unstable and stable plaque groups.

Item	Unstable plaque (n=17)	Stable plaque (n=25)	P-value
≥1 antiplatelet agent	15/17	24/25	0.556
≥1 antihypertensive agent	7/17	7/25	0.508
≥1 lipid-lowering agent	16/17	10/25	<0.001
≥1 glucose-lowering agent	3/17	4/25	>0.999
≥1 anticoagulant agent	0	0	
Quitting smoking	0	0	
CEA/CAS	0	0	
Outcome of stroke or TIA	2/17	2/25	>0.999
Ischemic stroke	2/17	2/25	
TIA	0	0	
Intracranial hemorrhage	0	0	

CEA, carotid endarterectomy; CAS, carotid artery stenting; TIA, transient ischemic stroke.

instance, along with the Reynolds risk score (22), the addition of Hs-CRP as well as family history and traditional risk factors was reported to efficiently improve the overall future risk prediction of cardiovascular events (23). However, further studies are required to address these issues.

To date, limited data are available concerning the roles of MCP-1 in vulnerable carotid plaques. Of note, in an *in vivo* animal study on apolipoprotein $E^{-/-}$ mice, site-specific delivery of adenoviral-mediated small hairpin RNA targeting mouse MCP-1 downregulated MCP-1 expression, which turned a vulnerable plaque into a more stable plaque phenotype and prevented plaque disruption, suggesting its detrimental effects on plaque stability (24). In parallel with these findings, the present study suggested that patients with unstable plaques had higher serum MCP-1 levels than patients with stable plaques or NCs. Together with the ROC analysis of calcium content or spectral curve slope, the present findings strongly suggest that MCP-1 may potentially be involved in carotid plaque instability and therefore utilized for the assessment of plaque vulnerability.

Although CT is relatively inexpensive as compared to MRI, the ionizing radiation of CT scanning has raised increasing concern in recent years. To reduce the risk of CT radiation, two strategies are proposed: One is justification, which refers to CT scans only when medically necessary; another is optimization, which refers to adjusting and operating a CT scanner to obtain images adequate for diagnosis at the lowest possible dose. Considering the great potential of GSI in detecting carotid atherosclerotic plaque components, appropriate use on patients requiring screening is thought to be necessary and beneficial. In addition, compared to conventional CT, the dose of X-ray radiation and contrast agent is decreased since GSI may achieve comparable contrast-to-noise ratios with lower dose efficiency. In any case, when choosing to perform CTA, the most suitable patients should be selected to gain the greatest benefit with minimum risk (25).

In the present study, although the incidence of ischemic stroke in the unstable plaque group was slightly higher than that in the stable plaque group (11.8 vs. 8.0%), no statistically significant difference was observed between these two groups during the 1-year follow-up, possibly due to the better compliance in the administration of lipid-lowering drugs in the former group (26). However, the association between these two GSI parameters and the risk of ischemic stroke was not investigated in the present study, mainly due to the small sample size and a short-term follow-up (at 1 year). However, a multicenter prospective study using a larger sample size will help determine the role of plaque features by GSI as possible clinical predictors of future ipsilateral cerebrovascular events.

In conclusion, the present study suggested that patients with unstable plaque exhibited a significantly lower calcium content and higher spectral curve slope than those of the stable plaque group. A marked alteration in GSI calcium content and spectral curve slope in patients with unstable plaque was observed, reflecting a close link between calcification and plaque instability. These two imaging parameters are of powerful diagnostic value in the determination of unstable plaques with different threshold values, indicating that they may serve as valuable biomarkers related to atherosclerosis and plaque vulnerability in clinical practice. However, the small sample size is a major limitation of the present study and larger-scale comparisons with histopathological specimens are required to validate the reliability of GSI-based CT carotid plaque imaging in the future. The present study also demonstrated altered serum levels of Hs-CRP and MCP-1 proteins in patients with unstable plaques, as well as their optimal diagnostic threshold values for determining unstable plaques, thus supporting the hypothesis that these pro-inflammatory molecules may be implicated in the process of plaque instability and may therefore serve as potential serological biomarkers for the prediction of vulnerable carotid plaques. In summary, the present findings support the feasibility of using these serological and imaging parameters as multiple potential biomarkers relevant to plaque vulnerability or stroke progression. However, these findings of GSI calcium content and spectral curve slope in vulnerable carotid plaques pave the way for identifying valuable candidate biomarkers in atherothrombotic stroke and for exploring novel therapeutic strategies for effective stroke prevention.

Acknowledgements

Not applicable.

Funding

No funding was received.

Availability of data and materials

The datasets used and/or analyzed during the current study are available from the corresponding author on reasonable request.

Authors' contributions

GZL and LW conceived the experiments. ZXF, XQL, TTY and KS performed the experiments. SJY, TTN and LM analyzed the results. ZXF and GZL confirm the authenticity of all the raw data. All authors have read and approved the final manuscript.

Ethics approval and consent to participate

The Ethics Review Board of Beijing Anzhen Hospital (Beijing, China) examined and approved the study protocol in accordance with the Declaration of Helsinki. Informed consent was obtained from all individual participants included in the study.

Patient consent for publication

Not applicable.

Competing interests

The authors declare that they have no competing interests.

References

1. Brinjikji W, Huston J III, Rabinstein AA, Kim GM, Lerman A and Lanzino G: Contemporary carotid imaging: From degree of stenosis to plaque vulnerability. J Neurosurg 124: 27-42, 2016.
2. Gao T, Zhang Z, Yu W, Zhang Z and Wang Y: Atherosclerotic carotid vulnerable plaque and subsequent stroke: A high-resolution MRI study. Cerebrovasc Dis 27: 345-352, 2009.
3. Takaya N, Yuan C, Chu B, Saam T, Underhill H, Cai J, Tran N, Polissar NL, Isaac C, Ferguson MS, *et al*: Association between carotid plaque characteristics and subsequent ischemic cerebrovascular events: A prospective assessment with MRI-initial results. Stroke 37: 818-823, 2006.
4. Stary HC, Chandler AB, Dinsmore RE, Fuster V, Glagov S, Insull W Jr, Rosenfeld ME, Schwartz CJ, Wagner WD and Wissler RW: A definition of advanced types of atherosclerotic lesions and a histological classification of atherosclerosis. A report from the committee on vascular lesions of the council on arteriosclerosis, American heart association. Circulation 92: 1355-1374, 1995.
5. Lusis AJ: Atherosclerosis. Nature 407: 233-241, 2000.
6. Moriya J. Critical roles of inflammation in atherosclerosis. J Cardiol 73: 22-27, 2019.
7. Tatsugami F, Higaki T, Nakamura Y, Honda Y and Awai K: Dual-energy CT: Minimal essentials for radiologists. Jpn J Radiol: Jan 4, 2022 (Epub ahead of print)..
8. Lorsakul A, Fakhri GE, Worstell W, Ouyang J, Rakvongthai Y, Laine AF and Li Q: Numerical observer for atherosclerotic plaque classification in spectral computed tomography. J Med Imaging (Bellingham) 3: 035501, 2016.
9. Shinohara Y, Sakamoto M, Kuya K, Kishimoto J, Yamashita E, Fujii S, Kurosaki M and Ogawa T: Carotid plaque evaluation using gemstone spectral imaging: Comparison with magnetic resonance angiography. J Stroke Cerebrovasc Dis 26: 1535-1540, 2017.
10. Shinohara Y, Sakamoto M, Kuya K, Kishimoto J, Iwata N, Ohta Y, Fujii S, Watanabe T and Ogawa T: Assessment of carotid plaque composition using fast-kV switching du-al-energy CT with gemstone detector: Comparison with extracorporeal and virtual histology-intravascular ultra-sound. Neuroradiology 57: 889-895, 2015.
11. Touboul PJ, Hennerici MG, Meairs S, Adams H, Amarenco P, Bornstein N, Csiba L, Desvarieux M, Ebrahim S, Hernandez Hernandez R, *et al*: Mannheim carotid intima-media thickness and plaque consensus (2004-2006-2011). An update on behalf of the advisory board of the 3rd, 4th and 5th watching the risk symposia, at the 13th, 15th and 20th European stroke conferences, Mannheim, Germany, 2004, Brussels, Belgium, 2006, and Hamburg, Germany, 2011. Cerebrovasc Dis 34: 290-296, 2012.
12. Ma G, Yu Y, Duan H, Dou Y, Jia Y, Zhang X, Yang C, Chen X, Han D, Guo C and He T: Subtraction CT angiography in head and neck with low radiation and contrast dose dual-energy spectral CT using rapid kV-switching technique. Br J Radiol 91: 20170631, 2018.
13. Motoyama S, Kondo T, Sarai M, Sugiura A, Harigaya H, Sato T, Inoue K, Okumura M, Ishii J, Anno H, *et al*: Multislice computed tomographic characteristics of coronary lesions in acute coronary syndromes. J Am Coll Cardiol 50: 319-326, 2007.
14. Vancheri F, Longo G, Vancheri S, Danial JSH and Henein MY: Coronary artery microcalcification: Imaging and clinical implications. Diagnostics (Basel) 9: 125, 2019.
15. Yue D, Li Fei S, Jing C, Ru Xin W, Rui Tong D, Ai Lian L and Luo YH: The relationship between calcium (water) density and age distribution in adult women with spectral CT: Initial result compared to bone mineral density by dual-energy X-ray absorptiometry. Acta Radiol 60: 762-768, 2019.
16. Kwee RM: Systematic review on the association between calcification in carotid plaques and clinical ischemic symptoms. J Vasc Surg 51: 1015-1025, 2010.
17. Barrett HE, Van der Heiden K, Farrell E, Gijsen FJH and Akyildiz AC: Calcifications in atherosclerotic plaques and impact on plaque biomechanics. J Biomech 87: 1-12, 2019.
18. Karçaaltıncaba M and Aktaş A: Dual-energy CT revisited with multidetector CT: Review of principles and clinical applications. Diagn Interv Radiol 17: 181-194, 2011.
19. Piepoli MF, Hoes AW, Agewall S, Albus C, Brotons C, Catapano AL, Cooney MT, Corrà U, Cosyns B, Deaton C, *et al*: ESC scientific document group. 2016 European guidelines on cardiovascular disease prevention in clinical practice: The sixth joint task force of the European society of cardiology and other societies on cardiovascular disease prevention in clinical practice (constituted by representatives of 10 societies and by invited experts) developed with the special contribution of the European association for cardiovascular prevention and rehabilitation (EACPR). Eur Heart J 37: 2315-2381, 2016.
20. Cimmino G, Ragni M, Cirillo P, Petrillo G, Loffredo F, Chiariello M, Gresele P, Falcinelli E and Golino P: C-reactive protein induces expression of matrix metalloproteinase-9: A possible link between inflammation and plaque rupture. Int J Cardiol 168: 981-986, 2013.
21. Nederkoorn PJ: Vulnerable carotid plaque and biomarkers: Multiplying individual risk profiles? Eur J Neurol 26: 1425, 2019.
22. Ridker PM, Buring JE, Rifai N and Cook NR: Development and validation of improved algorithms for the assessment of global cardiovascular risk in women: The reynolds risk score. JAMA 297: 611-619, 2007.
23. Emerging Risk Factors Collaboration, Kaptoge S, Di Angelantonio E, Pennells L, Wood AM, White IR, Gao P, Walker M, Thompson A, Sarwar N, *et al*: C-reactive protein, fibrinogen, and cardiovascular disease prediction. N Engl J Med 367: 1310-1320, 2012.
24. Liu XL, Zhang PF, Ding SF, Wang Y, Zhang M, Zhao YX, Ni M and Zhang Y: Local gene silencing of monocyte chemoattractant protein-1 prevents vulnerable plaque disruption in apolipoprotein E-knockout mice. PLoS One 7: e33497, 2012.
25. Schmidt CW: CT scans: Balancing health risks and medical benefits. Environ Health Perspect 120: A118-A121, 2012.
26. Amarenco P, Bogousslavsky J, Callahan A III, Goldstein LB, Hennerici M, Rudolph AE, Sillesen H, Simunovic L, Szarek M, Welch KM, *et al*: High-dose atorvastatin after stroke or transient ischemic attack. N Engl J Med 355: 549-559, 2006.